Penetration Landing Guidance Trajectories in the Presence of Windshear

A. Miele* and T. Wang†
Rice University, Houston, Texas
and
W. W. Melvin‡
Delta Airlines, Atlanta, Georgia

This paper is concerned with the guidance of flight trajectories in the presence of windshear. The penetration landing problem is considered with reference to flight in a vertical plane. In addition to the horizontal shear, the presence of a downdraft is assumed. First, the optimal trajectory is determined by minimizing a performance index measuring the deviation of the flight trajectory from the nominal trajectory, subject to touchdown constraints, under the assumption that two controls are available, the angle of attack and the power setting. Also, a quasioptimal trajectory is determined under the assumption that only one control is available, the angle of attack; the power setting is specified in advance, based on the optimal trajectory results. Numerical experiments indicate that the quasioptimal trajectory is close to the optimal trajectory. Next, a guidance scheme is constructed in which the angle of attack is determined by the windshear intensity, the absolute path inclination, and the glide slope angle, whereas the power setting is determined by the windshear intensity and the velocity. Finally, for low-altitude penetration landing, a simplified guidance scheme is constructed by controlling the angle of attack via absolute path inclination signals, while keeping the power setting at the maximum permissible value after the windshear is detected. Numerical experiments indicate that the guidance trajectories are close to the optimal trajectory.

Nomenclature

C_D = drag coefficient
C_L = lift coefficient
D = drag force, lb
g = acceleration of gravity, ft/s^2
h = altitude, ft
L = lift force, lb
m = mass, lb s^2/ft
S = reference surface area, ft^2
T = thrust force, lb
V = relative velocity, fps
W = mg = weight, lb
W_h = h-component of wind velocity, fps
W_x = x-component of wind velocity, fps
x = horizontal distance, ft
α = relative angle of attack, rad
β = engine power setting
γ = relative path inclination, rad
γ_e = absolute path inclination, rad
γ_g = glide slope inclination, rad
δ = thrust inclination, rad
θ = pitch attitude angle (wing), rad
λ = wind intensity parameter
ρ = air density, lb s^2/ft^4
τ = final time, s

Received Jan. 25, 1988; revision received July 15, 1988; presented as Paper 88-4069 at the AIAA Guidance, Navigation, and Control Conference, Minneapolis, MN, Aug. 15-17, 1988.

*Foyt Family Professor of Aerospace Sciences and Mathematical Sciences, Aero-Astronautics Group. Fellow AIAA.
†Senior Research Scientist, Aero-Astronautics Group. Member AIAA.
‡Captain; Chairman, Airworthiness and Performance Committee, Air Line Pilots Association, Washington, DC. Member AIAA.

I. Introduction

LOW-ALTITUDE windshear is a threat to the safety of aircraft in takeoff and landing.[1] Over the past 20 years, some 30 aircraft accidents have been attributed to windshear. The most notorious ones are the crash of PAN AM Flight 759 on July 9, 1982, at New Orleans International Airport (Boeing B-727, in takeoff[2]) and the crash of Delta Airlines Flight 191 on August 2, 1985, at Dallas-Fort Worth International Airport (Lockheed L-1011, in landing[3-5]).

Low-altitude windshear is usually associated with a severe meteorological phenomenon, called the downburst. In turn, a downburst involves a descending column of air, which then spreads horizontally in the neighborhood of the ground. This condition is hazardous, because an aircraft in takeoff or landing might encounter a head wind coupled with a downdraft, followed by a tail wind coupled with a downdraft. Hence, an inadvertent encounter with a low-altitude windshear can be a serious problem for even a skilled pilot.

This paper is concerned with the penetration landing problem.[6,7] When the pilot of an aircraft on a glide path detects an encounter with a low-altitude windshear, he must choose between abort landing[8-10] and penetration landing.[11-15] Clearly, if the initial altitude is high enough, abort landing is a safer procedure than penetration landing; on the other hand, if the initial altitude is low enough, the opposite might be true. In low-altitude penetration landing, the aircraft might have to traverse only a part of the shear region; in low-altitude abort landing, the aircraft might have to traverse the whole of the shear region.

When studying the penetration landing problem one can take two points of view: optimization and guidance. In optimization studies,[6] one assumes that global information on the wind flowfield is available and determines the optimal trajectory, namely, the flight trajectory minimizing a suitable performance index, while satisfying the constraining relations. In guidance studies,[7] one assumes that only local information on the wind flowfield is available and determines a near-optimal trajectory, namely, a trajectory that approximates the behavior of the optimal trajectory.

To sum up, this paper deals with the guidance of penetration landing trajectories in the presence of windshear. We consider flight in a vertical plane, governed by either two controls (the angle of attack and the power setting) or one control (the angle of attack, if the power setting is predetermined). We impose inequality constraints on the angle of attack, the power setting, and their time derivatives. Also, we impose the following requirements:

1) The absolute path inclination at touchdown is to be -0.5 deg.

2) The velocity at touchdown is to be within 30 knots of the nominal value.

3) The horizontal distance at touchdown is to be within 1000 ft of the nominal value.

4) The deviation of the flight trajectory from the nominal trajectory is to be small.

Under these constraints, we determine the control distribution that minimizes a performance index measuring the deviation of the flight trajectory from the nominal trajectory. In turn, the nominal trajectory includes two parts: the approach part, in which the absolute path inclination is constant, and the flare part, in which the absolute path inclination is a linear function of the horizontal distance.

We close this introduction by noting that the present paper is part of a comprehensive research program undertaken at Rice University on optimal trajectories, guidance schemes, and piloting strategies for takeoff, abort landing, and penetration landing. For previous studies of optimal trajectories and guidance schemes for takeoff and abort landing, see Refs. 8-10 and 16-21.

For the penetration landing problem, an important difference between this paper and Refs. 11-15 must be noted. In Refs. 11-15, attention was focused on only the approach path, with the intent of satisfying requirement 4. In this paper, attention is focused on both the approach path and the flare path, with the intent of statisfying all four requirements.

Not only is this larger number of requirements significant from a flight mechanics point of view, but also from a control point of view. Indeed, in standard control practice,[22,23] the number of required outputs is usually equal to the number of controls (in the present case, two). If the number of required outputs exceeds the number of controls, the design of guidance and control systems becomes considerably more complicated.

II. Equations of Motion

We make use of the relative wind-axes system in connection with the following assumptions: 1) the aircraft is a particle of constant mass; 2) flight takes place in a vertical plane; 3) Newton's law is valid in an Earth-fixed system; and 4) the wind flowfield is steady.

With the preceding premises, the equations of motion include the kinematical equations

$$\dot{x} = V\cos\gamma + W_x \tag{1a}$$

$$\dot{h} = V\sin\gamma + W_h \tag{1b}$$

and the dynamical equations

$$\dot{V} = (T/m)\cos(\alpha+\delta) - D/m - g\sin\gamma - (\dot{W}_x\cos\gamma + \dot{W}_h\sin\gamma) \tag{2a}$$

$$\dot{\gamma} = (T/mV)\sin(\alpha+\delta) + L/mV - (g/V)\cos\gamma + (1/V)(\dot{W}_x\sin\gamma - \dot{W}_h\cos\gamma) \tag{2b}$$

Because of assumption 4, the total derivatives of the wind velocity components and the corresponding partial derivatives satisfy the relations

$$\dot{W}_x = (\partial W_x/\partial x)(V\cos\gamma + W_x) + (\partial W_x/\partial h)(V\sin\gamma + W_h) \tag{3a}$$

$$\dot{W}_h = (\partial W_h/\partial x)(V\cos\gamma + W_x) + (\partial W_h/\partial h)(V\sin\gamma + W_h) \tag{3b}$$

These equations must be supplemented by the functional relations

$$T = T(h,V,\beta) \tag{4a}$$

$$D = D(h,V,\alpha), \qquad L = L(h,V,\alpha) \tag{4b}$$

$$W_x = W_x(x,h), \qquad W_h = W_h(x,h) \tag{4c}$$

and by the analytical relations

$$\gamma_e = \arctan[(V\sin\gamma + W_h)/(V\cos\gamma + W_x)] \tag{5a}$$

$$\theta = \alpha + \gamma \tag{5b}$$

For a given value of the thrust inclination δ, the differential system [Eqs.(1-4)] involves four state variables [the horizontal distance $x(t)$, the altitude $h(t)$, the velocity $V(t)$, and the relative path inclination $\gamma(t)$] and two control variables [the angle of attack $\alpha(t)$ and the power setting $\beta(t)$]. However, the number of control variables reduces to one (the angle of attack), if the power setting is specified in advance. The quantities defined by the analytical relations (5) can be computed a posteriori, once the values of the state and the control are known.

Angle of Attack Bounds

The angle of attack α and its time derivative $\dot{\alpha}$ are subject to the inequalities

$$\alpha \le \alpha_*, \qquad -\dot{\alpha}_* \le \dot{\alpha} \le \dot{\alpha}_* \tag{6}$$

where α_* is a prescribed upper bound and $\dot{\alpha}_*$ is a prescribed, positive constant.

For the guidance trajectories, inequalities (6) are enforced directly. For the optimal trajectories, inequalities (6) are enforced indirectly via the following transformation technique:

$$\alpha = \alpha_* - u^2 \tag{7a}$$

$$\dot{u} = -(\dot{\alpha}_*/2u)\sin\phi, \qquad |u| \ge \epsilon \tag{7b}$$

$$\dot{u} = -(\dot{\alpha}_*/2u)\sin^2(\pi u/2\epsilon)\sin\phi, \qquad |u| \le \epsilon \tag{7c}$$

Here, $u(t)$, $\phi(t)$ are auxiliary variables and ϵ is a small, positive constant that is introduced to prevent the occurrence of boundary singularities. Note that the right-hand sides of Eqs. (7b) and (7c) are continuous and have continuous first derivatives at $|u| = \epsilon$. Clearly, when using Eqs. (7) in conjunction with Eqs. (1-4), one must regard $\alpha(t)$, $u(t)$ as state variables and $\phi(t)$ as a control variable.

Power Setting Bounds

The power setting β and its time derivative $\dot{\beta}$ are subject to the inequalities

$$\beta_* \le \beta \le 1, \qquad -\dot{\beta}_* \le \dot{\beta} \le \dot{\beta}_* \tag{8}$$

where β_* is a prescribed lower bound and $\dot{\beta}_*$ is a prescribed, positive constant.

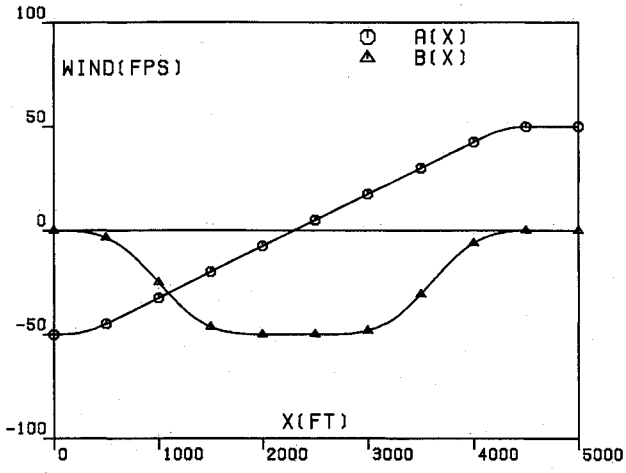

Fig. 1 Horizontal wind function $A(x)$ and vertical wind function $B(x)$.

For the guidance trajectories, inequalities (8) are enforced directly. For the optimal trajectories, inequalities (8) are satisfied directly if the power setting is specified in advance. On the other hand, if the power setting is not specified in advance [that is, if $\beta(t)$ is regarded as a control], it is convenient to rewrite inequalities (8) in the form

$$\beta \geq \beta_* \tag{9a}$$

$$\beta \leq 1 \tag{9b}$$

$$-\dot{\beta}_* \leq \dot{\beta} \leq \dot{\beta}_* \tag{9c}$$

Then, inequality (9a) is enforced indirectly via a penalty function technique, whereas inequalities (9b) and (9c) are enforced indirectly via the following transformation technique, which is analogous to that described by Eqs. (7):

$$\beta = 1 - w^2 \tag{10a}$$

$$\dot{w} = -(\dot{\beta}_*/2w)\sin\psi, \qquad |w| \geq \eta \tag{10b}$$

$$\dot{w} = -(\dot{\beta}_*/2w)\sin^2(\pi w/2\eta)\sin\psi, \qquad |w| \leq \eta \tag{10c}$$

Here, $w(t)$, $\psi(t)$ are auxiliary variables and η is a small, positive constant, which is introduced to prevent the occurrence of boundary singularities. Note that the right-hand sides of Eqs. (10b) and (10c) are continuous and have continuous first derivatives at $|w| = \eta$. Clearly, when using Eqs. (10) in conjunction with Eqs. (1-4), one must regard $\beta(t)$, $w(t)$ as state variables and $\psi(t)$ as a control variable.

III. System Description

The numerical examples of this paper refer to a Boeing B-727 aircraft powered by three JT8D-17 turbofan engines. It is assumed that the runway is located at sea-level altitude; the ambient temperature is 100°F; the gear is down; the flap setting is $\delta_F = 30$ deg; the landing weight is $W = 150{,}000$ lb.

Thrust

The dependence of the thrust on the altitude is disregarded, and the function (4a) is written as

$$T = \beta T_*(V) \tag{11}$$

The reference thrust $T_*(V)$ is given in Fig. 1a of Ref. 6. The power setting β is subject to inequalities (8), with $\beta_* = 0.2$ and $\dot{\beta}_* = 0.3$/s.

Aerodynamic Forces

The dependence of the drag and the lift on the altitude is disregarded, and the functions (4b) are written as

$$D = (1/2)C_D(\alpha)\rho S V^2, \qquad L = (1/2)C_L(\alpha)\rho S V^2 \tag{12}$$

The drag coefficient $C_D(\alpha)$ is given in Fig. 1b of Ref. 6, and the lift coefficient $C_L(\alpha)$ is given in Fig. 1c of Ref. 6. The angle of attack α is subject to inequalities (6), with $\alpha_* = 17.2$ deg and $\dot{\alpha}_* = 3.0$ deg/s.

Wind Model

The dependence of the horizontal wind on the altitude is disregarded, and the functions (4c) are written as

$$W_x = \lambda A(x), \qquad W_h = \lambda(h/h_*)B(x) \tag{13a}$$

with

$$\lambda = \Delta W_x/\Delta W_{x*} \tag{13b}$$

The function $A(x)$ represents the distribution of the horizontal wind vs the horizontal distance (Fig. 1); the function $B(x)$ represents the distribution of the vertical wind vs the horizontal distance (Fig. 1); the parameter λ characterizes the intensity of the shear/downdraft combination; ΔW_x is the horizontal wind velocity difference (maximum tail wind minus maximum head wind); $\Delta W_{x*} = 100$ fps is a reference value for the horizontal wind velocity difference; and $h_* = 1000$ ft is a reference value for the altitude.

The one-parameter family of wind models [Eqs. (13)] has the following properties:

1) It represents the transition from a uniform head wind to a uniform tail wind, with nearly constant shear in the core of the downburst.

2) The downdraft achieves maximum negative value at the center of the downburst.

3) The downdraft vanishes at $h = 0$.

4) The functions W_x, W_h nearly satisfy the continuity equation and the irrotationality condition in the core of the downburst.

Decreasing values of λ correspond to milder windshears; conversely, increasing values of λ correspond to more severe windshears. If one excludes the 1983 windshear episode at Andrews Air Force Base, the highest value of λ ever recorded is $\lambda = 1.40$, corresponding to $\Delta W_x = 140$ fps. Hence, in this paper, the following values of λ are considered:

$$\lambda = 1.0, \quad 1.2, \quad 1.4 \tag{14a}$$

corresponding to

$$\Delta W_x = 100, \quad 120, \quad 140 \text{ fps} \tag{14b}$$

For additional information concerning wind models, see Refs. 24 and 25.

Initial Conditions

For the examples of this paper, the following initial conditions are assumed:

$$x_0 = 0 \text{ ft} \tag{15a}$$

$$h_0 = 200, \quad 600, \quad 1000 \text{ ft} \tag{15b}$$

$$V_0 = V_{\text{ref}} + 10 \text{ knots} = 142 \text{ knots} \tag{15c}$$

$$\gamma_{e0} = -3.0 \text{ deg} \tag{15d}$$

The initial values γ_0, α_0, θ_0, β_0 are computed using Eqs. (15) and the assumption of quasisteady flight prior to the windshear onset.

Final Conditions

Concerning the altitude at touchdown, the following value is assumed:

$$h_\tau = 0 \text{ ft} \tag{16}$$

For both the guidance trajectories and the optimal trajectories, Eq. (16) determines indirectly the final time τ, which is free.

Concerning the absolute path inclination at touchdown, the following value is assumed:

$$\gamma_{e\tau} = -0.5 \text{ deg} \tag{17a}$$

For the optimal trajectories, precise satisfaction of Eq. (17a) is required. For the guidance trajectories, Eq. (17a) is replaced with the double inequality

$$-1.0 \leq \gamma_{e\tau} \leq 0.0 \text{ deg} \tag{17b}$$

whose satisfaction is achieved via the structure of the guidance scheme.

Concerning the velocity at touchdown, the following inequality is assumed:

$$V_\ell \leq V_\tau \leq V_u \tag{18a}$$

The lower bound V_ℓ, the upper bound V_u, and the nominal velocity at touchdown $\tilde{V}_\tau$ are given by[6,7]

$$V_\ell = \tilde{V}_\tau - 30 \text{ knots} = 112 \text{ knots} \tag{18b}$$

$$V_u = \tilde{V}_\tau + 30 \text{ knots} = 172 \text{ knots} \tag{18c}$$

$$\tilde{V}_\tau = V_0 = 142 \text{ knots} \tag{18d}$$

The lower bound [Eq. (18b)] is determined by the fact that, if the velocity is too low, it is difficult to control the trajectory in such a way that the touchdown path inclination requirement [Eq. (17a) or (17b)] can be met. The upper bound [Eq.(18c)] is determined by the need for containing the runway length needed for depleting the velocity to zero after touchdown. For the optimal trajectories, inequality (18a) is enforced indirectly via a penalty function technique and/or via the trigonometric transformation

$$V_\tau = (V_\ell + V_u)/2 + [(V_u - V_\ell)/2] \sin p \tag{18e}$$

where p denotes a parameter to be determined. For the guidance trajectories, satisfaction of inequality (18a) is achieved via the structure of the guidance scheme.

Concerning the distance at touchdown, the following inequality is assumed:

$$x_\ell \leq x_\tau \leq x_u \tag{19a}$$

The lower bound x_ℓ, the upper bound x_u, and the nominal distance at touchdown $\tilde{x}_\tau$ are given by[6,7]

$$x_\ell = \tilde{x}_\tau - 1000 \text{ ft} \tag{19b}$$

$$x_u = \tilde{x}_\tau + 1000 \text{ ft} \tag{19c}$$

$$\tilde{x}_\tau = (h_f - h_0)/\tan\gamma_{e0} - 2h_f/(\tan\gamma_{e0} + \tan\gamma_{e\tau}) = 19.1h_0 + 682 \text{ ft} \tag{19d}$$

Here, h_0 is the initial altitude; $h_f = 50$ ft is the altitude at the end of the approach path/beginning of the flare path; $\gamma_{e0} = -3.0$ deg is the absolute path inclination at the initial point; and $\gamma_{e\tau} = -0.5$ deg is the absolute path inclination at touchdown.

The bounds [Eqs. (19b) and (19c)] are determined by the need of avoiding excessive undershooting/overshooting of the nominal touchdown distance. For the optimal trajectories, inequality (19a) is enforced indirectly via a penalty function technique and/or via the trigonometric transformation

$$x_\tau = (x_\ell + x_u)/2 + [(x_u - x_\ell)/2] \sin q \tag{19e}$$

where q denotes a parameter to be determined. For the guidance trajectories, satisfaction of inequality (19a) is achieved via the structure of the guidance scheme.

Nominal Trajectory

In the absence of windshear, the geometry of a nominal landing trajectory $\tilde{h}(x)$ can be computed, based on simple assumptions on the distribution of slopes. Let the nominal glide path be subdivided into an approach path and a flare path. Assume that the slope of the approach path is constant and that the slope of the flare path is a linear function of the horizontal distance. Upon integration, one sees that the function $\tilde{h}(x)$ is described by a linear relation for the approach path and a quadratic relation for the flare path (see Refs. 6–7 for details).

IV. Optimal Trajectories

Optimal trajectories can be generated by assuming that two controls are available: the angle of attack $\alpha(t)$ and the power setting $\beta(t)$. For this problem, the feasibility relations include: the state equations (1–4); the inequality constraints (6), converted into equality constraints by means of Eqs. (7); the inequality constraints (9b) and (9c), converted into equality constraints by means of Eqs. (10); the initial conditions (15); the final conditions (16) and (17a); and the inequality constraints (18a) and (19a), converted into equality constraints by means of Eqs. (18e) and (19e). The power setting constraint (9a), omitted from the feasibility relations, is reintroduced into the problem via a penalty term.

The preceding system includes eight state variables [$x(t)$, $h(t)$, $V(t)$, $\gamma(t)$, $\alpha(t)$, $u(t)$, $\beta(t)$, $w(t)$], two control variables [$\phi(t)$, $\psi(t)$], and three parameters (p, q, τ). With this understanding, we formulate the following Bolza problem [problem (P)]: Subject to the previous constraints, minimize the functional

$$I = (1/\tau h_*^2)\int_0^\tau [h - \tilde{h}(x)]^2 dt - (1/\tau)\int_0^\tau K_1(\beta - 1.5\beta_*)^3 dt - (1/\tau V_*^3)\int_0^\tau K_2(V_0 - V)^3 dt + (K_3/V_*^2)(V_\tau - \tilde{V}_\tau)^2 + (K_4/x_*^2)(x_\tau - \tilde{x}_\tau)^2 \tag{20}$$

Here, τ is the flight time; $h_* = 1000$ ft is a reference altitude; $V_* = V_0$ is a reference velocity; and $x_* = 1000$ ft is a reference distance. The penalty coefficients have the following values:

$$K_1 = 0, \quad \text{if } \beta - 1.5\beta_* \geq 0 \tag{21a}$$

$$K_1 = 100, \quad \text{if } \beta - 1.5\beta_* < 0 \tag{21b}$$

$$K_2 = 0, \quad \text{if } V_0 - V \geq 0 \tag{21c}$$

$$K_2 = 1, \quad \text{if } V_0 - V < 0 \tag{21d}$$

$$K_3 = 0.02\, h/h_* \tag{21e}$$

$$K_4 = 0.02\, h/h_* \tag{21f}$$

The functional (20) is the sum of a basic quadratic term, two cubic penalty terms, and two quadratic penalty terms. The basic quadratic term measures the deviation of the flight trajectory from the nominal trajectory. The first cubic penalty term forces the satisfaction of inequality (9a); the second cubic penalty term avoids excessive overshooting of the velocity V_0 along the trajectory. The first quadratic penalty term forces the touchdown velocity to be near its nominal value; the second quadratic penalty term forces the touchdown distance to be near its nominal value.

With reference to Eqs. (20) and (21), the following comments are in order:

1) The weighting factor 1.5 in the power setting term ensures

that the lower boundary for the power setting is not undershot.

2) Strictly speaking, the presence of the last two terms in Eq. (20) is not necessary, owing to the use of Eqs. (18e) and (19e). In practice, such presence leads to touchdown values for the velocity and the distance that are close to the nominal values.

V. Quasioptimal Trajectories

Quasioptimal trajectories can be generated by assuming that only one control is available, the angle of attack $\alpha(t)$, under the assumption that the power setting $\beta(t)$ is given. For this problem, the feasibility relations include: the state equations (1-4); the inequality constraints (6), converted into equality constraints by means of Eqs. (7); the initial conditions (15); and the final conditions (16) and (17a). The inequality constraints (18a) and (19a), omitted from the feasibility relations, are reintroduced into the problem via penalty terms.

The preceding system includes six state variables $[x(t), h(t), V(t), \gamma(t), \alpha(t), u(t)]$, one control variable $[\phi(t)]$, and one parameter (τ). With this understanding, we formulate the following Bolza problem [problem (Q)]: Subject to the previous constraints, minimize the functional

$$I=(1/\tau h_*^2)\int_0^\tau [h-\tilde{h}(x)]^2 dt+(K_3/V_*^2)(V_\tau-\tilde{V}_\tau)^2 + (K_4/x_*^2)(x_\tau-\tilde{x}_\tau)^2 \tag{22}$$

The penalty coefficients have the following values:

$$K_3=0.002 \tag{23a}$$

$$K_4=0.002 \tag{23b}$$

The functional (22) is the sum of a basic quadratic term and two quadratic penalty terms. The basic quadratic term measures the deviation of the flight trajectory from the nominal trajectory. The first quadratic penalty term forces the touchdown velocity to be near its nominal value; the second quadratic penalty term forces the touchdown distance to be near its nominal value.

If we compare problem (P) with problem (Q), we see that the latter differs from the former in four ways:

1) Equations (10), which account for the inequality constraints (9b) and (9c), are excluded from the feasibility relations.

2) The cubic penalty term, which accounts for the inequality constraint (9a), is excluded from the objective functional.

3) The cubic penalty term, which avoids excessive overshooting of the velocity V_0, is excluded from the objective functional.

4) Equations (18e) and (19e), which force the satisfaction of the inequality constraints (18a) and (19a), are excluded.

The common reason for these differences is that the presence of such terms is rendered unnecessary by the assumed power setting $\beta(t)$. More specifically, the power setting $\beta(t)$, derived from the analysis of the results pertaining to the optimal trajectories of Sec. IV, is described as follows:

1) For the shear portion of the trajectory, the maximum power setting is maintained; that is, the function $\beta(t)$ is given by

$$\beta=\beta_0+\dot{\beta}_0 t, \qquad 0\le t\le\sigma \tag{24a}$$

$$\beta=1, \qquad \sigma\le t\le\omega \tag{24b}$$

with $\sigma=(1-\beta_0)/\dot{\beta}_0$. Here, $t=0$ is the initial time, $t=\sigma$ is the time at which the maximum power setting is reached, and $t=\omega$ is the time at which the shear terminates; also, β_0 is the initial power setting, and $\dot{\beta}_0$ is the initial time rate of increase of the power setting, chosen to be $\dot{\beta}_0=0.2/\text{s}$.

2) For the aftershear portion of the trajectory, the maximum power setting is maintained if $V\le V_\ell$ and the reduced power setting is maintained if $V>V_\ell$; that is, $\beta(t)$ is supplied by the following relationship:

$$\beta-\beta_0=-[(1-\beta_0)/(V_0-V_\ell)](V-V_0) \tag{25a}$$

$$\beta_*\le\beta\le 1, \qquad \omega\le t\le\tau \tag{25b}$$

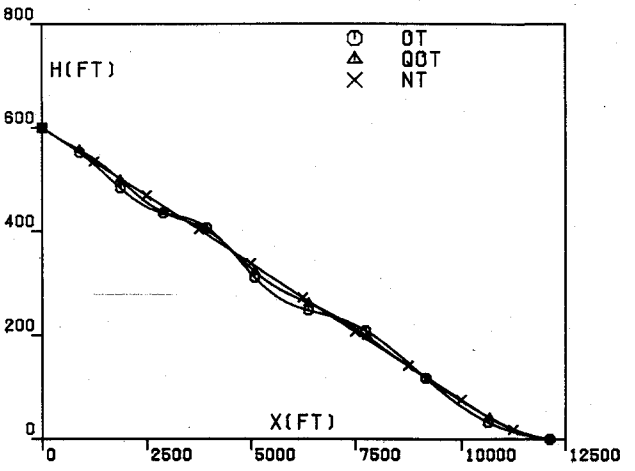

Fig. 2a Optimal trajectories, $h_0=600$ ft, $\lambda=1.2$: altitude h vs distance x.

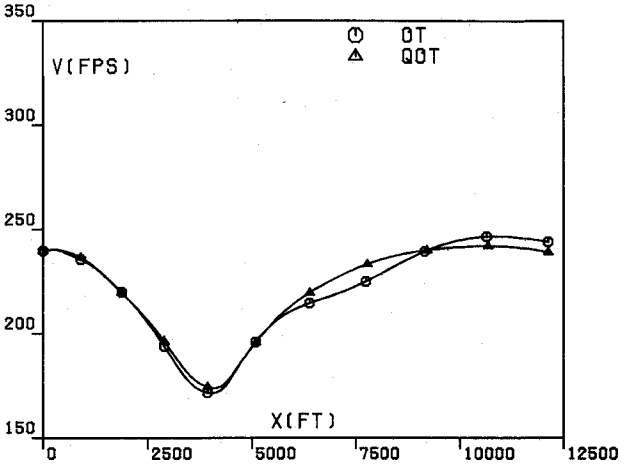

Fig. 2b Optimal trajectories, $h_0=600$ ft, $\lambda=1.2$: relative velocity V vs distance x.

VI. Numerical Results for Optimal Trajectories

Problems (P) and (Q) were solved with the sequential gradient-restoration algorithm, employed in conjunction with the primal formulation (PSGRA).[26,27] Computations were performed at Rice University using an NAS-AS-9000 computer. Several combinations of initial altitude and windshear intensity were considered, specifically:

$$h_0=200,\ 600,\ 1000 \text{ ft} \tag{26a}$$

$$\lambda=1.0,\ 1.2,\ 1.4 \tag{26b}$$

For a particular case, namely, $h_0=600$ ft and $\lambda=1.2$, the numerical results are presented in Fig. 2. This figure includes four parts: the altitude h (Fig. 2a); the relative velocity V (Fig. 2b); the relative angle of attack α (Fig. 2c); and the power setting β (Fig. 2d). For more detailed results, see Ref. 7.

From the numerical results, upon comparing the optimal trajectory (OT), the quasioptimal trajectory (QOT), and the nominal trajectory (NT), certain general conclusions become apparent:

1) The OT and the QOT are geometrically close to one another, and both are close to the NT.

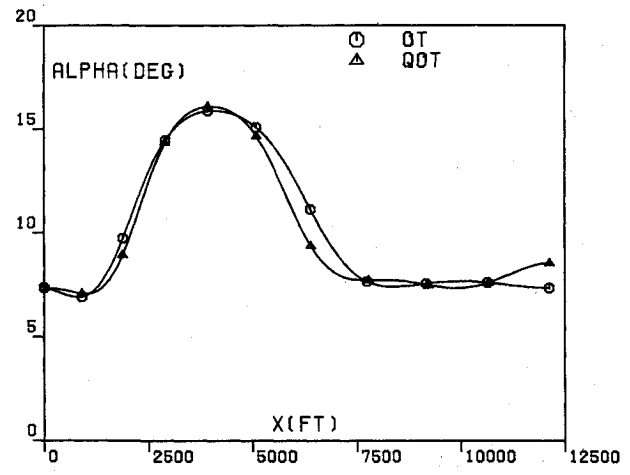

Fig. 2c Optimal trajectories, $h_0 = 600$ ft, $\lambda = 1.2$: angle of attack α vs distance x.

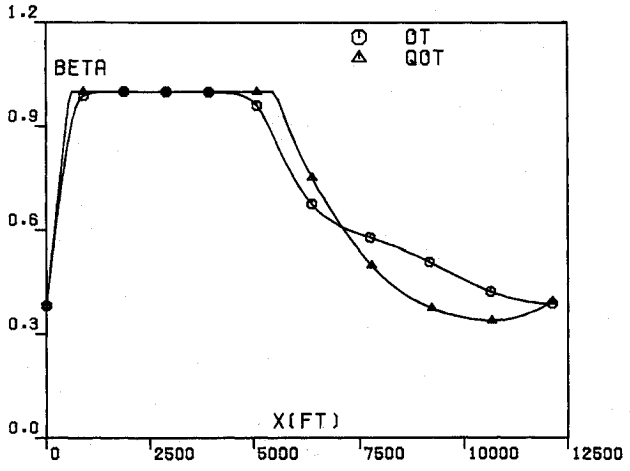

Fig. 2d Optimal trajectories, $h_0 = 600$ ft, $\lambda = 1.2$: power setting β vs distance x.

2) Both the OT and the QOT satisfy the touchdown requirements concerning the absolute path inclination, the velocity, and the distance.

With particular reference to strong-to-severe windshears, the OT and the QOT exhibit the following characteristics:

1) The angle of attack has an initial decrease, which is followed by a gradual, sustained increase. The largest value of the angle of attack is attained near the end of the shear; in the aftershear region, the angle of attack decreases gradually.

2) Initially, the power setting increases at a nearly constant time rate until the maximum power setting is reached; then, the maximum power setting is maintained in the shear region. In the aftershear region, the power setting decreases gradually.

3) The relative velocity decreases in the shear region and increases in the aftershear region. The point of minimum velocity occurs at the end of the shear.

4) Depending on the initial altitude and the windshear intensity, the deviations of the flight trajectory from the nominal trajectory can be considerable in the shear region; however, these deviations become small in the aftershear region, and the flight trajectory recovers the nominal trajectory.

The comparative numerical results of this section show that the OT of problem (P) and the QOT of problem (Q) are close to one another. This implies that, for the purposes of constructing a guidance scheme, the coupling relation between the angle of attack and the power setting can be ignored. This separation result simplifies to a considerable degree the design of guidance and control systems capable of approximating the behavior of the optimal penetration landing trajectory in the presence of windshear.

VII. Guidance Trajectories

In this section, we present a guidance scheme whose objective is to approximate the behavior of the optimal penetration landing trajectory in a windshear. Whereas the optimal trajectory is based on global information on the wind distribution, the guidance scheme relies on local information on the horizontal wind acceleration $\dot{W}_x$, the downdraft W_h, and the state of the aircraft. In constructing the guidance scheme, the following points must be kept in mind:

1) The guidance scheme is to be such that requirements 1–4 of Sec. I are met.

2) Although the requirements are four, only two controls are available, namely, the angle of attack and the power setting.

3) Based on the separation result established in Sec. VI, the guidance law for the angle of attack can be constructed independently of the guidance law for the power setting.

4) The guidance law for the power setting is to be such that requirement 2 of Sec. I is met.

5) The guidance law for the angle of attack is to be such that requirements 1, 3, and 4 of Sec. I are met.

6) Since satisfying requirement 4 implies satisfying requirement 3, the guidance law for the angle of attack can be reduced to taking care of only two essential requirements, namely, requirements 1 and 4 of Sec. I.

Power Setting

For the power setting, the guidance law must be such that the maximum power setting is maintained in the shear portion of the trajectory and velocity recovery is ensured in the aftershear portion. With reference to strong-to-severe windshears, the analytical form of the guidance law is given as follows:

Shear portion:

$$\beta = 1 \tag{27a}$$

Aftershear portion:

$$V = V_0 \tag{27b}$$

In feedback control form, Eqs. (27) can be implemented as follows:

$$\beta - \beta_0 = -K_1(V - V_0) + K_2 F \tag{28a}$$

$$F = \dot{W}_x/g - W_h/V \tag{28b}$$

$$K_1 = (1 - \beta_0)/(V_0 - V_\ell) \tag{28c}$$

$$K_2 = (1 - \beta_0)/F_c \tag{28d}$$

$$\beta_* \le \beta \le 1, \quad -\dot{\beta}_* \le \dot{\beta} \le \dot{\beta}_* \tag{28e}$$

Here, β is the instantaneous power setting and $\beta_0 = 0.3330$ is the nominal power setting in the absence of windshear; V is the instantaneous velocity, V_0 is the nominal velocity, and V_ℓ is the lower bound for the velocity; F is the shear/downdraft factor, introduced in Ref. 18, and $F_c = 0.1250$ is a critical value for the shear/downdraft factor; K_1 is the gain coefficient for velocity error and K_2 is the shear/downdraft gain coefficient. For the assumed values of β_0, V_0, V_ℓ, F_c, the gain coefficients take the following values:

$$K_1 = 0.01316 \text{ s/ft} \tag{29a}$$

$$K_2 = 5.336 \tag{29b}$$

The power setting feedback control law [Eqs. (28)] employs both velocity signals and windshear signals. Concerning the windshear signals, note that the power setting response is such that, as F increases, the value of β increases, tending to the maximum value $\beta = 1$ as F reaches the critical value F_c.

Angle of Attack

For the angle of attack, the guidance law must be such that, if there is no windshear or if the windshear is weak, the absolute path inclination γ_e is constant along the approach path and is nearly linear with the altitude along the flare path. Under the same conditions, the glide slope γ_g is constant along the approach path ($\gamma_g = \gamma_{e0} = -3.0$ deg). Note that the glide slope is not defined along the flare path. On the other hand, if the windshear is strong-to-severe, the values of the absolute path inclination and the glide slope must be corrected for windshear effects, which increase as the shear/downdraft factor and the altitude increase. This is suggested by the results of Sec. VI on optimal and quasioptimal trajectories.

With the preceding understanding, the analytical form of the guidance law is given by

$$\gamma_e = \tilde{\gamma}_e(h,F) \tag{30a}$$

$$\tilde{\gamma}_e = \gamma_{e0} - \mu, \qquad h \geq h_f \tag{30b}$$

$$\tilde{\gamma}_e = \gamma_{e0} h/h_f + \gamma_{er}(1 - h/h_f), \qquad h \leq h_f \tag{30c}$$

$$\mu = 0, \qquad F \leq F_c \text{ or } h \leq h_f \tag{30d}$$

$$\mu = 0.002(1 - F_c/F)(h/h_f - 1), \qquad F \geq F_c \text{ and } h \geq h_f \tag{30e}$$

and

$$\gamma_g = \tilde{\gamma}_g(h,F) \tag{31a}$$

$$\tilde{\gamma}_g = \gamma_{e0} + \mu, \qquad h \geq h_f \tag{31b}$$

$$\mu = 0, \qquad F \leq F_c \text{ or } h \leq h_f \tag{31c}$$

$$\mu = 0.002(1 - F_c/F)(h/h_f - 1), \qquad F \geq F_c \text{ and } h \geq h_f \tag{31d}$$

Here, Eqs. (30) refer to the absolute path inclination and Eqs.(31) refer to the glide slope. The terms $-\mu$ and $+\mu$ represent the corrections to the absolute path inclination and the glide slope due to windshear effects. These corrections vanish for weak-to-moderate windshears and lower altitudes; they become increasingly larger for strong-to-severe windshears and higher altitudes.

In feedback control form, Eqs. (30) and (31) can be implemented as follows:

$$\alpha - \tilde{\alpha}(V) = -K_3[\gamma_e - \tilde{\gamma}_e(h,F)] - K_4[\gamma_g - \tilde{\gamma}_g(h,F)] \tag{32a}$$

$$K_3 = 5 \tag{32b}$$

$$K_4 = 5(h/h_f - 1), \qquad h \geq h_f \tag{32c}$$

$$K_4 = 0, \qquad h \leq h_f \tag{32d}$$

$$\alpha \leq \alpha_*, \qquad -\dot{\alpha}_* \leq \dot{\alpha} \leq \dot{\alpha}_* \tag{32e}$$

Here, α is the instantaneous angle of attack and $\tilde{\alpha}(V)$ is the nominal angle of attack[18]; γ_e is the instantaneous absolute path inclination and $\tilde{\gamma}_e(h,F)$ is the nominal absolute path inclination [Eqs. (30)]; γ_g is the instantaneous glide slope and $\tilde{\gamma}_g(h,F)$ is the nominal glide slope [Eqs. (31)]; h is the instantaneous altitude and $h_f = 50$ ft is the altitude at the end of the approach path/beginning of the flare path; K_3 is the gain coefficient for absolute path inclination error and K_4 is the gain coefficient for glide slope error.

The angle of attack feedback control law [Eqs. (32)] employs absolute path inclination signals, glide slope signals, and windshear signals. The function of the absolute path inclination signals is to make sure that the touchdown absolute path inclination requirement [inequality (17b)] is met. The function of the glide slope signals is to make sure that the guidance trajectory is geometrically close to the nominal trajectory. The function of the windshear signals is to contain the velocity loss due to windshear action by allowing more altitude loss at higher altitudes; hence, at lower altitudes, sufficient velocity is available so that the aircraft can be controlled effectively.

The gain coefficients are adjusted in such a way that their ratio is given by

$$K_4/K_3 = h/h_f - 1, \qquad h \geq h_f \tag{33a}$$

$$K_4/K_3 = 0, \qquad h \leq h_f \tag{33b}$$

Clearly, when computing the values of the angle of attack via Eqs. (32), the glide slope signals are predominant at higher altitudes (approach path), whereas the absolute path inclination signals are predominant at lower altitudes (flare path). In this way, both the absolute path inclination requirement [Eq. (17a)] and the distance requirement [inequality (19a)] can be met.

VIII. Simplified Guidance Trajectories

From a practical point of view, it must be emphasized that penetration landing makes sense only if the windshear encounter occurs at lower altitudes; if the windshear encounter occurs at higher altitudes, abort landing must be preferred. Therefore, low-altitude penetration landing deserves particular attention. For this special situation, the guidance scheme of Sec. VII can be simplified by keeping the power setting at the maximum permissible value and by controlling the angle of attack via absolute path inclination signals.

Power Setting

For low-altitude penetration landing, the power setting is given by the analytical relations

$$\beta = \beta_0 + \dot{\beta}_0 t, \qquad 0 \leq t \leq \sigma \tag{34a}$$

$$\beta = 1, \qquad \sigma \leq t \leq \tau \tag{34b}$$

with $\sigma = (1 - \beta_0)/\dot{\beta}_0$. Here, β is the instantaneous power setting, β_0 is the initial power setting, $\dot{\beta}_0$ is the constant time rate of increase of the power setting, σ is the time at which maximum power setting is reached, and τ is the final time.

Strictly speaking, Eqs. (34) apply only to the shear portion of the trajectory. However, for low-altitude penetration landing, Eqs. (34) apply also to the aftershear portion of the trajectory, since the time span corresponding to the aftershear portion is small. In the aftershear portion, the power setting must be kept at the maximum value $\beta = 1$, since the velocity at the end of the shear is lower than V_0, and hence a velocity increase is necessary.

Angle of Attack

For low-altitude penetration landing, the analytical form of the guidance law is given by

$$\gamma_e = \tilde{\gamma}_e(h) \tag{35a}$$

$$\tilde{\gamma}_e = \gamma_{e0}, \qquad h \geq h_f \tag{35b}$$

$$\tilde{\gamma}_e = \gamma_{e0} h/h_f + \gamma_{er}(1 - h/h_f), \qquad h \leq h_f \tag{35c}$$

In feedback control form, Eqs. (35) can be implemented as follows:

$$\alpha - \tilde{\alpha}(V) = -K_3[\gamma_e - \tilde{\gamma}_e(h)] \tag{36a}$$

$$K_3 = 5 \tag{36b}$$

$$\alpha \leq \alpha_*, \qquad -\dot{\alpha}_* \leq \dot{\alpha} \leq \dot{\alpha}_* \tag{36c}$$

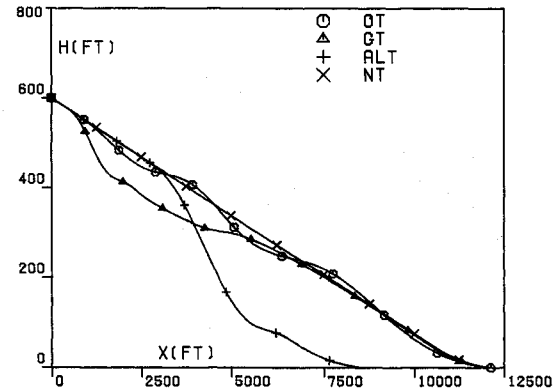

Fig. 3a Guidance trajectories, $h_0 = 600$ ft, $\lambda = 1.2$: altitude h vs distance x.

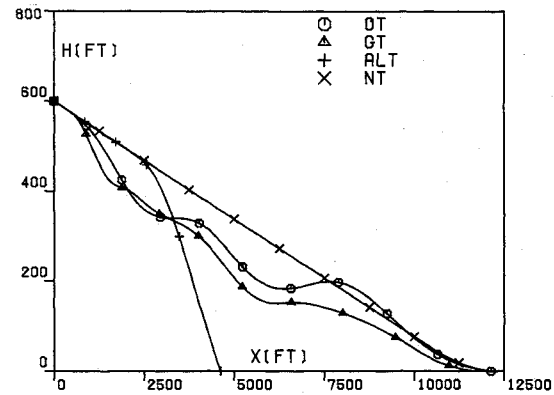

Fig. 3b Guidance trajectories, $h_0 = 600$ ft, $\lambda = 1.4$: altitude h vs distance x.

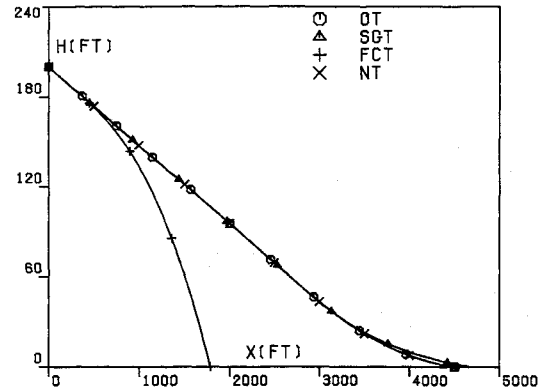

Fig. 4a Guidance trajectories, $h_0 = 200$ ft, $\lambda = 1.2$: altitude h vs distance x.

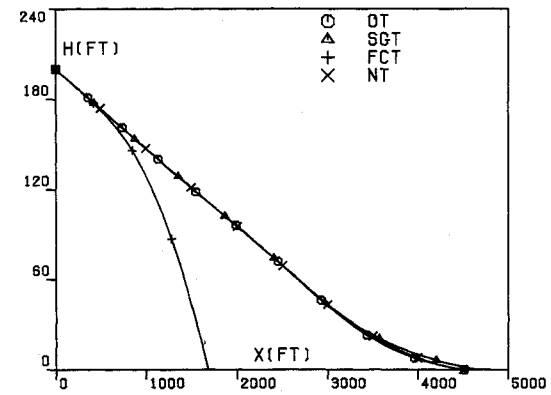

Fig. 4b Guidance trajectories, $h_0 = 200$ ft, $\lambda = 1.4$: altitude h vs distance x.

Here, α is the instantaneous angle of attack and $\tilde{\alpha}(V)$ is the nominal angle of attack[18]; γ_e is the instantaneous absolute path inclination and $\tilde{\gamma}_e(h)$ is the nominal absolute path inclination [Eqs. (35)]; h is the instantaneous altitude and $h_f = 50$ ft is the altitude at the end of the approach path/beginning of the flare path; K_3 is the gain coefficient for absolute path inclination error.

Comparing the feedback control law [Eqs. (32)] and the simplified feedback control law [Eqs. (36)], we see that both the glide slope signals and the windshear signals are being ignored. At lower altitudes, ignoring the glide slope signals is permissible in view of Eqs. (33). At lower altitudes, ignoring the windshear signals is also permissible, since the windshear signals are small and priority must be given to achieving the absolute path inclination necessary for safe touchdown.

IX. Numerical Results for Guidance Trajectories

In this section, we compare the following trajectories: the NT of Sec. III, the OT of Sec. IV, the GT of Sec. VII, and the SGT of Sec. VIII. Also, we consider two alternative trajectories, described below: the fixed control trajectory (FCT) and the autoland trajectory (ALT).

The fixed control trajectory is obtained by keeping constant both the power setting and the angle of attack. Therefore, it is described by

$$\beta = \beta_0 \tag{37a}$$

$$\alpha = \alpha_0 \tag{37b}$$

where β_0, α_0 denote prewindshear values.

The autoland trajectory is obtained by controlling the power setting via velocity signals and the angle of attack via absolute path inclination signals. Therefore, it is described by the following feedback control laws:

$$\beta - \beta_0 = -K_2(V - V_0) \tag{38a}$$

$$K_2 = (1 - \beta_0)/(V_0 - V_t) \tag{38b}$$

$$\beta_* \le \beta \le 1, \qquad -\dot{\beta}_* \le \dot{\beta} \le \dot{\beta}_* \tag{38c}$$

and

$$\alpha - \tilde{\alpha}(V) = -K_3[\gamma_e - \tilde{\gamma}_e(h)] \tag{39a}$$

$$\tilde{\gamma}_e = \gamma_{e0}, \qquad h \ge h_f \tag{39b}$$

$$\tilde{\gamma}_e = \gamma_{e0} h/h_f + \gamma_{er}(1 - h/h_f), \qquad h \le h_f \tag{39c}$$

$$K_3 = 5 \tag{39d}$$

$$\alpha \le \alpha_*, \qquad -\dot{\alpha}_* \le \dot{\alpha} \le \dot{\alpha}_* \tag{39e}$$

The comparison of trajectories is done in terms of the ability to meet the path inclination, velocity, and distance requirements at touchdown. Several combinations of initial altitude and windshear intensity are considered, specifically:

$$h_0 = 200, \quad 600, \quad 1000 \text{ ft} \tag{40a}$$

$$\lambda = 1.0, \quad 1.2, \quad 1.4 \tag{40b}$$

For the particular case $h_0 = 600$ ft, comparative numerical results concerning the functions $h(t)$ of the OT, the GT, and the ALT are presented in Fig. 3. This figure includes two parts: Fig. 3a refers to $\lambda = 1.2$, and Fig. 3b refers to $\lambda = 1.4$. For the particular case $h_0 = 200$ ft, comparative numerical results concerning the functions $h(t)$ of the OT, the SGT, and the FCT are presented in Fig. 4. This figure includes two parts: Fig. 4a refers to $\lambda = 1.2$, and Fig. 4b refers to $\lambda = 1.4$. For more detailed results, see Ref. 7.

From the numerical results, upon comparing the FCT, the ALT, the GT, the SGT, the OT, and the NT, certain general conclusions become apparent.

1) The FCT is unable to meet the specified touchdown requirements. This statement holds regardless of the initial altitude and the windshear intensity.

2) The ALT is able to meet the specified touchdown requirements for weak-to-moderate windshears, but not for strong-to-severe windshears. For severe windshears, an undesirable characteristic of the ALT is that the point of minimum velocity occurs before the end of the shear. The velocity increase in the windshear region is coupled with severe altitude loss, occasionally resulting in a crash.

3) The GT is close to the OT, especially for strong-to-severe windshears. For these windshears, the GT has better survival capability than the ALT. The superiority of the GT over the ALT is due particularly to the fact that the point of minimum velocity of the GT occurs at the end of the shear (as in the OT), whereas this is not the case with the ALT.

4) The GT exhibits relatively large oscillations of the angle of attack. These oscillations can be smoothed by employing some more sophisticated feedback control design than the simple proportional feedback control employed in this paper.

5) At lower altitudes, the SGT is close to the OT, especially for strong-to-severe windshears.

X. Conclusions

The penetration landing problem in the presence of windshear is considered with reference to flight in a vertical plane. Attention is focused on the minimization of the deviation of the flight trajectory from the nominal trajectory, subject to touchdown constraints. The optimal trajectory is determined by controlling both the angle of attack and the power setting. Also, a quasioptimal trajectory is determined by controlling only the angle of attack, subject to a power setting law derived from the optimal trajectory study. This leads to a separation result for the control of angle of attack and power setting.

The aforementioned separation result simplifies to a considerable degree the design of guidance and control systems capable of approximating the behavior of the optimal trajectory. In the guidance scheme, the angle of attack is determined by the windshear intensity, the absolute path inclination, and the glide slope angle, whereas the power setting is determined by the windshear intensity and the velocity. Also, for low-altitude penetration landing, a simplified guidance scheme is constructed by controlling the angle of attack via absolute path inclination signals, while keeping the power setting at the maximum permissible value after the windshear is detected. Numerical experiments indicate that the guidance trajectories are close to the optimal trajectory, which in turn is close to the nominal trajectory.

In closing, the following remarks are pertinent:

1) While the results of this paper have been obtained by using the angle of attack as a control variable, they also could have been obtained by using the pitch angle as a control variable. Indeed, the transformation $\alpha = \theta - \gamma$ allows one to replace α with θ, if so desired [see Eq. (5b)].

2) In this paper, the point-mass model has been employed in connection with flight in a vertical plane [see Eqs. (1-4)]. Future investigations might include the consideration of additional factors such as the rotational motion of the aircraft, the presence of crosswinds and cross shears, the presence of ground effects, and so on.

Acknowledgments

This research was supported by the NASA Langley Research Center (NASA-LRC), Grant NAG-1-516, by the Boeing Commercial Airplane Company (BCAC), and by the Air Line Pilots Association. The authors are indebted to Dr. R. L. Bowles (NASA-LRC) and Dr. G. R. Hennig (BCAC) for helpful discussions.

References

[1]Fujita, T. T., *The Downburst,* Dept. of Geophysical Sciences, Univ. of Chicago, Chicago, IL, 1985.

[2]"Pan American World Airways, Clipper 759, Boeing 727-235, N4737, New Orleans International Airport, Kenner, LA, July 9, 1982," National Transportation Safety Board, Aircraft Accident Rept. 8302, 1983.

[3]"Delta Air Lines, Lockheed L-1011-3851, N726DA, Dallas-Fort Worth International Airport, TX, Aug. 2, 1985," National Transportation Safety Board, Aircraft Accident Rept. 8605, 1986.

[4]Fujita, T. T., *DFW Microburst,* Dept. of Geophysical Sciences, Univ. of Chicago, Chicago, IL, 1986.

[5]Gorney, J. L., "An Analysis of the Delta 191 Windshear Accident," AIAA Paper 87-0626, 1987.

[6]Miele, A., Wang, T., Wang, H., and Melvin, W. W., "Optimal Penetration Landing Trajectories in the Presence of Windshear," AIAA Paper 88-0580, 1988.

[7]Miele, A., Wang, T., and Melvin, W. W., "Penetration Landing Guidance Trajectories in the Presence of Windshear," Rice Univ., Houston, TX, Aero-Astronautics Rept. 218, 1987.

[8]Miele, A., Wang. T., Tzeng, C. Y., and Melvin, W. W., "Transformation Techniques for Minimax Optimal Control Problems and Their Application to Optimal Flight Trajectories in a Windshear: Optimal Abort Landing Trajectories," International Federation of Automatic Control, Paper 87-9221, 1987.

[9]Miele, A., Wang, T., Tzeng, C. Y., and Melvin, W. W., "Optimization and Guidance of Abort Landing Trajectories in a Windshear," AIAA Paper 87-2341, 1987.

[10]Miele, A., Wang, T., and Melvin, W. W., "Acceleration, Gamma, and Theta Guidance Schemes for Abort Landing Trajectories in the Presence of Windshear," Rice Univ., Houston, TX, Aero-Astronautics Rept. 223, 1987.

[11]Frost,W., "Flight in Low Level Windshear," NASA CR 3678, 1983.

[12]Psiaki, M. L. and Stengel, R. F., "Analysis of Aircraft Control Strategies for Microburst Encounter," AIAA Paper 84-0238, 1984.

[13]Psiaki, M. L. and Stengel, R. F., "Optimal Flight Paths Through Microburst Wind Profiles," *Journal of Aircraft,* Vol. 23, Aug. 1986, pp. 629-635.

[14]Chu, P. Y. and Bryson, A. E., Jr., "Control of Aircraft Landing Approach in Windshear," AIAA Paper 87-0632, 1987.

[15]Hahn, K. Y., "Take-Off and Landing in a Downburst," International Council of the Aeronautical Sciences, Paper 86-562, 1986.

[16]Miele, A., Wang, T., and Melvin, W. W., "Optimal Take-Off Trajectories in the Presence of Windshear," *Journal of Optimization Theory and Applications,* Vol. 49, April 1986, pp. 1-45.

[17]Miele, A., Wang, T., and Melvin, W. W., "Guidance Strategies for Near-Optimum Take-Off Performance in a Windshear," *Journal of Optimization Theory and Applications,* Vol. 50, July 1986, pp. 1-47.

[18]Miele, A., Wang, T., and Melvin, W. W., "Optimization and Acceleration Guidance of Flight Trajectories in a Windshear," *Journal of Guidance, Control, and Dynamics,* Vol. 10, July-Aug. 1987, pp. 368-377.

[19]Miele, A., Wang, T., Melvin, W. W., and Bowles, R. L., "Gamma Guidance Schemes for Flight in a Windshear," *Journal of Guidance, Control, and Dynamics,* Vol. 11, July-Aug. 1988, pp. 320-327.

[20]Miele, A., Wang, T., Melvin, W. W., and Bowles, R. L., "Maximum Survival Capability of an Aircraft in a Severe Windshear," *Journal of Optimization Theory and Applications,* Vol. 53, May 1987, pp. 181-217.

[21]Miele, A., Wang. T., and Melvin, W. W., "Quasisteady Flight to Quasisteady Flight Transition in a Windshear: Trajectory Optimization and Guidance," *Journal of Optimization Theory and Applications,* Vol. 54, Aug. 1987, pp. 203-240.

[22]Callier, F. M. and Desoer, C. A., *Multivariable Feedback Systems,* Springer-Verlag, New York, 1982.

[23]Franklin, G. F., Powell, J. D., and Emani-Naeini, A., *Feedback Control of Dynamic Systems,* Addison-Wesley, Reading, MA, 1986.

[24]Ivan, M., "A Ring-Vortex Downburst Model for Flight Simulation," *Journal of Aircraft,* Vol. 23, March 1986, pp. 232-236.

[25]Wingrove, R. C. and Bach, R. E., Jr., "Severe Winds in the DFW Microburst Measured from Two Aircraft," AIAA Paper 87-2340, 1987.

[26]Miele, A. and Wang, T., "Primal-Dual Properties of Sequential Gradient-Restoration Algorithms for Optimal Control Problems, Part 1, Basic Problem," *Integral Methods in Science and Engineering,* edited by F. R. Payne et al., Hemisphere, Washington, DC, 1986, pp. 577-607.

[27]Miele, A. and Wang, T., "Primal-Dual Properties of Sequential Gradient-Restoration Algorithms for Optimal Control Problems, Part 2, General Problem," *Journal of Mathematical Analysis and Applications,* Vol. 119, Oct.-Nov. 1986, pp. 21-54.